Original
ISSN 2413-0516

Discovery of New Thiourea Derivatives as Potential SIRT Inhibitors

Mohammed Abdullah Abbas[1], Ayad A. Al-Hamashi[2*]

[1]Department of Pharmaceutical Chemistry, College of Pharmacy, University of Baghdad, Bab-Almoadham, Baghdad 10047, Iraq.
*Correspondence to: Ayad A. Al-Hamashi (E-mail: a.alhamashi@ccopharm.uobaghdad.edu.iq)
(Submitted: 18 July 2024 – Revised version received: 11 August 2024 – Accepted: 29 August 2024 – Published online: 26 October 2024)

Abstract
Objective: This study aimed to design and synthesize novel thiourea-based compounds targeting Sirtuins (SIRTs), a class of histone deacetylase enzymes implicated in various cellular processes, including cancer, and to evaluate their cytotoxic potential against colon cancer cells.
Methods: Virtual modeling and molecular docking studies were conducted to design the compounds and assess their interaction with SIRT enzymes. Compounds showing acceptable docking scores were selected for organic synthesis. The final compounds (MA-1 to MA-6) were synthesized and characterized using FTIR, ^{1}H-NMR, and ^{13}C-NMR spectroscopy. Cytotoxicity studies were performed on SW480 colon cancer cells to evaluate the biological activity of the synthesized compounds.
Results: All synthesized compounds exhibited promising cytotoxicity against SW480 colon cancer cells, with MA-2 demonstrating a particularly strong effect. The half-maximal inhibition concentration (IC50) of the compounds was in the single-digit micromolar range, comparable to established SIRT inhibitors Selisistat and AGK2.
Conclusion: The thiourea-based compounds synthesized in this study, especially MA-2, showed significant potential as SIRT inhibitors with cytotoxic activity against colon cancer cells. These results warrant further investigation into their therapeutic potential.
Keywords: Sirtuin, thiourea, molecular docking, colon cancer

Introduction

Cancer is one of the leading causes of death. It is characterized by uncontrolled cell growth which leads to various complications.[1] Despite the advances in cancer treatment strategies, developing selective and potent molecules to tackle cancer progression is still needed.[2,3] The definition of "Epigenetics" emerged as a heritable change in a chromosome without alteration in DNA sequence.[4] Histone acetylation is an essential epigenetic modification that indirectly controls gene transcription via two major enzymes, histone deacetylases (HDACs) and histone acetyltransferases (HATs).[5]

Carcinogenesis shows an overexpression of HDACs which makes them a promising target for HDAC inhibitors development.[6] Mammalian cells have been proven to contain 18 HDACs. Subsequently, these 18 mammalian HDACs have been divided into four specific classes (classes I, II, III, and IV) depending on multiple factors such as functional similarity, enzymatic activity, sequence homology, systematic analysis, and domain structure. Three of these classes need zinc for activity (class I, class II, and class IV), while the third class is NAD^{+} dependent HDAC enzymes that are subdivided into seven members of Sirtuins (SIRTs) 1–7.[7–9] SIRT proteins' importance lies in their involvement in many cellular functions and age-related disorders such as diabetes, cardiovascular disease, neurodegeneration, and multiple cancer types.[10,11] Most of the Sirtuin inhibitors are SIRT1 selective.[12] The first SIRT1 activator resveratrol **(I)** has been utilized as a lead compound for further investigation and research to create synthetic polyphenolic derivatives as SIRT1 activator. On the other hand, Selisistat (EX-527) **(II)** was utilized as the first effective SIRT1 inhibitor that reached clinical trials in the treatment of Huntington's disease (Figure 1).[13]

Numerous urea-containing compounds are utilized in clinic due to their ability to form stable interactions with the biological targets.[14] Research on cell biology revealed that when a particular thiourea derivative was present, cancer cells' ability to maintain the integrity of their plasma membrane was weakened. Because of their bio-acceptability, thiourea derivatives are a great source of safe and effective anticancer Agents.[15] In this work, several thiourea-based molecules with a potential SIRT inhibition activity were developed, and their preliminary cytotoxicity activity was assessed.

Materials and Methods

Materials and Equipment

Starting materials, reagents, and catalysts were provided by multiple commercial suppliers (Sigma Aldrich, Thomas Baker, Macklin, and Merk). All reaction solvents were anhydrous. Thin layer chromatography (TLC) silica gel (20*20 cm) of (60 F254) sheet supplied by Merk. Silica gel (60 mm–120 mm) for column chromatography, and ethyl acetate: n-hexane were used as solvent system. Melting points were examined using the Electro-Thermal capillary apparatus (Stuart SMP 30), and all readings were uncorrected. The FT-IR spectroscopy (Shimadzu, Japan). ^{1}H-NMR and ^{13}C-NMR analysis was performed using Bruker 400 MHz and 500 MHz-Avance III spectrometer (DMSO-*d6* as the solvent). Molecular modeling studies were performed using a licensed Schrödinger suite version 13.0.135 thhat embedded with Maestro software. The colon cancer (SW480) cell line was obtained from Lonza Biologics, UK.

Molecular Docking

The human SIRT1-3 crystal structures were downloaded from the protein data bank (PDB) 4I5I, 5YQO, and 4JT8.[16–18] All proteins were co-crystalized with a specific ligand and contained NAD+ in their core as a co-factor. Proteins underwent processing through the protein preparation wizard in Schrödinger software. The non-essential atoms and water were

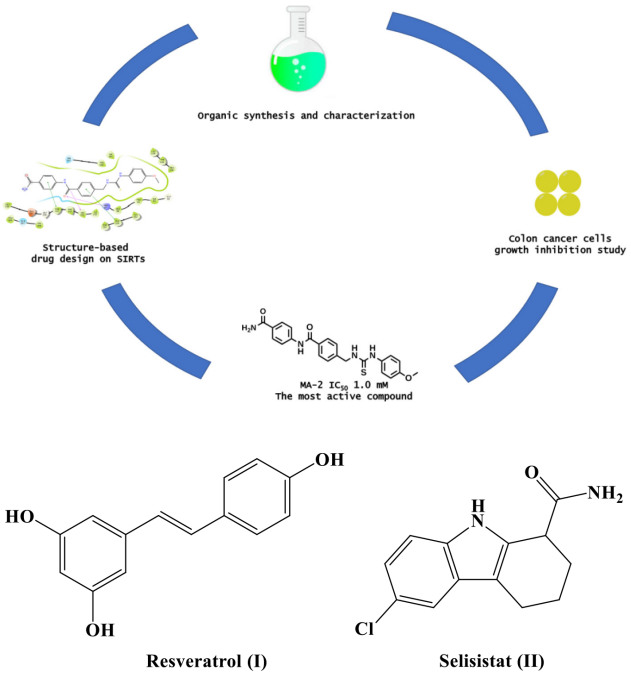

Fig. 1 **Structure of resveratrol and Selisistat.**

eliminated, and the proteins were optimized by the addition of missed atoms and hydrogen. The receptor grid was generated by centralizing the boundary box and positioning the ligand in the center. The used boundary box dimensions were 15 Å * 15 Å * 15 Å.[19,20] All ligands were built using Schrodinger's 2D structure builder, and then inserted into the prepared ligand module as input files. The ligands energy was minimized using the OLPS_2005 force field in Schrodinger LigPrep software.[19,21] The grid-based ligand docking (Glide) was used to conduct molecular docking studies using standard precision (SP) docking investigations to determine binding energies. Glide scoring function (G score) of the compounds was used for ranking ligands. ligand-binding geometries with SIRT proteins and potential energy predictions were utilized for evaluating the ligands. Sorting of compound poses was carried out regarding their respective scores and then visualized using Maestro interface.[22]

ADME Study

The absorption, distribution, metabolism, and elimination (ADME) study for compounds was performed in the licensed Schrödinger system using QIKPROP software to predict pharmacokinetic properties of the designed compounds with acceptable docking score and fitness to the receptors visually using default setup.[21,23,24]

Antiproliferative Study

The MTT study in this work was performed to evaluate cancer cell growth inhibition. Selisistat, AGK-2, and **MA1—MA6** were added and incubated into colon cancer (SW480) cells. The stock solution concentration used for references and final compounds was 0.1 mg/mL, and serial dilution by 50% for all compounds was performed (100, 50, 25, 12.5, 6.25, 0.313 µg/mL). 2 µL of each dilution was introduced into 198 µL of colon cancer cell line (SW480) and incubated for 24 h at 37 °C. The drug exposure period was completed after that, the medium was removed from wells, and phosphate buffer saline PBS for washing the cells. A blank control was used to affirm formazan residue formation, 1.2 mL from the solution of MTT (5 mg/L) was introduced to 10.8 mL of the medium to attain a concentration of 0.5 mg/L. Thereafter, filling each well with 200 µL of the resulting solution, and incubation of plate for 3 h at 37 °C until purple formazan crystals were viewed under an inverted microscope. 100 µL of DMSO was added to all of the wells after the supernatant was removed to dissolve the formazan crystals that resulted. Incubation of the plate was performed for half an hour at 25 °C until the purple crystals of formazan dissolved and the cell lysed. The percentage of proliferation was performed and calculated by multiplying the resulting number from the division of absorbance readings of test samples by control samples' readings.[25]

Results

Molecular Docking Study

The docking results for the synthesized compounds showed that the compounds have proper interaction with SIRT1-3 with acceptable docking scores (Table 1). A comprehensive analysis of the ligand orientation within the active site revealed an excellent alignment since the compounds are elegantly extended through the narrow channels of the enzyme, and the substituted aromatic fit outside the surface of the active site.

ADMET Study

The virtual prediction of pharmacokinetic parameters is a crucial step prior to synthesis and preclinical or preliminary works. The designed compounds must meet specific requirements in order to be regarded as drug-like molecules, including the percent of human oral absorption, number of rotating functional groups, rule of three, and rule of five. As a result, all compounds involved minimum violations of the Lipinski rule of five and Jorgensen's criteria rule of three, which might indicate that compounds have an acceptable drug-likeness profile (Table 2).

Chemistry

The convergent synthesis for the proposed compounds is commenced with the thiourea formation reaction between 4-(aminomethyl) benzoic acid (**III**) and 1-isothiocyanate-4 methoxybenzene (**IV**) to produce thiourea intermediate (**V**),[26]

Table 1. **The docking score for the binding of Selisistat, AGK2 and the designed compounds with SIRT1-3**

Code	Docking score (kcal/mol)		
	SIRT1	SIRT2	SIRT3
Selisistat	−9.45	−7.62	−7.49
AGK2	−5.05	−8.69	−7.28
MA1	−8.09	−8.30	−7.32
MA2	−6.49	−9.94	−8.30
MA3	−5.70	−8.77	−5.7
MA4	−7.01	−8.86	−6.65
MA5	−8.18	−9.24	−8.09
MA6	−6.9	−8.62	−8.26

Table 2. **Drug likeness properties of Selisistat, AGK2 and the designed compounds**

Code	Rule of Five	Rule of Three	CNS	#Metab	#rtvFG	% Human Oral Absorption
Selisistat	0	0	0	3	0	87.39
AGK2	1	1	0	2	1	96.27
MA1	1	1	−1	4	0	92.59
MA2	0	1	−2	3	0	84.82
MA3	1	1	0	4	0	92.63
MA4	1	1	−1	3	0	100.00
MA5	0	1	−1	3	0	100.00
MA6	0	1	−1	3	0	100.00

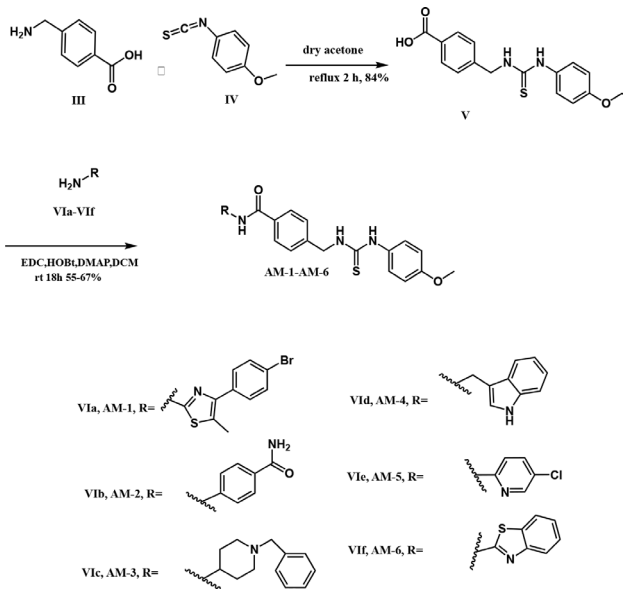

Scheme. 1 **Synthesis of final compounds.**

which followed by the amide bond formation reaction between compound **V** with various amine derivatives **VIa**—**VIf** to afford the final compounds **MA1**—**MA6** (Scheme 1).[27,28]

Synthesis of the thiourea intermediate (**V**)

To a mixture of 4-(aminomethyl) benzoic acid (**III**) (1.5 g, 10 mmol, 1 eq) in 30 mL of acetone was added 1-isothiocyanate-4 methoxybenzene (**IV**) (1.65 g, 10 mmol, 1 eq). The mixture was refluxed at 65°C for 2 h. Thereafter, the mixture was poured into a cold 5% HCl solution (30 mL) to produce a white precipitate which was filtered, dried, and purified by column chromatography using ethyl acetate: n-hexane to obtain a white powder of compound **V** in a yield (84%).[26,29] M.P. (206-209), FT-IR: broad (3271−2542), 3271, 3182, 3032, 2908, 2835, 1693, 1593, 1531, 1504, 1423, 1288, 1238, 1176 cm^{-1}. ^1H NMR (500 MHz, DMSO-*d6*) δ 9.51 (s, 1H, NH), 8.04 (s, 1H, NH), 7.89 (d, 2H, CH), 7.39 (d, 2H, CH), 7.23 (d, 2H, CH), 6.90 (d, 2H, CH), 4.77 (d, 2H, CH_2), 3.73 (s, 3H, CH_3). ^{13}C NMR (126 MHz, DMSO-*d6*) δ 181.80, 167.84, 157.22, 145.02, 131.95, 129.94, 129.74, 127.62, 126.73, 114.50, 55.71, 47.45.

General procedure for the synthesis of final compounds **(MA1—MA6).**

To a mixture of compound **V** (948 mg, 3 mmol, 1 eq) in 15 mL of dichloromethane (DCM) was separately added variant substituted amines (**VIa**—**VIf**) with equimolar amounts (3 mmol, 1 eq) to attain the final products. The selected amines for final compounds **(MA1**—**MA6)** are : [4-(4-bromophenyl)-5-methylthiazol-2-amine] (807 mg, 3 mmol)], [4-aminobenzamide (408 mg, 3 mmol)], [1-benzylpiperidin-4-amine (570 mg, 3 mmol)], [(1H-indol-3-yl)methanamine (438 mg, 3 mmol)], [5-chloropyridin-2-amine (483 mg, 3 mmol)], [benzo[d]thiazol-2-amine (450 mg, 3 mmol), were added individually. Then EDC.HCl (573 mg, 3 mmol, 1 eq), DMAP (366 mg, 3 mmol, 1 eq), HOBT (41 mg, 0.3 mmol, 0.1 eq), and DIPEA (775 mg, 6 mmol, 2 eq) were added. The mixture was stirred for 2 h at 0° C and then at room temperature for 18 h. After completion, the mixture was extracted from 10 mL of 5% HCl and 10 mL of 10% sodium bicarbonate ($NaHCO_3$). The organic layer was concentrated, and the residue was purified using column chromatography (ethyl acetate: n-hexane).[28]

N-(4-(4-bromophenyl)-5-methylthiazol-2-yl)-4-((3-(4-methoxyphenyl) thioureido) methyl) benzamide **(MA1)**

Yellow powder in a yield (55%), M.P**.** (170−173), FT-IR: 3375, 3159, 2954, 2924, 2854, 1658, 1608, 1535, 1508, 1284, 1246, 1168 cm^{-1}, ^1H NMR (500 MHz, DMSO-*d6*) δ 12.59 (s, 1H, NH), 9.50 (s, 1H, NH), 8.05 (d, 1H, NH), 7.80 – 7.52 (m, 6H, CH), 7.44 (d, 2H, CH), 7.24 (d, 2H, CH), 6.91 (d, 2H, CH), 4.80 (d, 2H, CH_2), 3.73 (s, 6H, CH_3).

N-(4-carbamoylphenyl)-4-((3-(4-methoxyphenyl) thioureido) methyl) benzamide **(MA2)**

Off white powder in a yield (64%), M.P. (194−197), FT-IR: 3290, 3259, 3055, 2924, 2835, 1651, 1531, 1508, 1269, 1242, 1168 cm^{-1}, ^1H NMR (500 MHz, DMSO-*d6*) δ 10.07 (s, 1H, NH), 9.48 (s, 1H, NH), 8.02 (s, 1H, NH), 7.89 (d, 2H, CH), 7.65 (d, 2H, CH), 7.42 (d, 2H, CH), 7.24 (d, 2H, CH), 6.91 (d, 4H, CH), 4.79 (s, 2H, CH_2), 3.73 (s, 3H, CH_3). ^{13}C NMR (126 MHz, DMSO-*d6*) δ 181.78, 165.45, 157.26, 156.00, 143.49, 133.89, 132.67, 131.93, 127.97, 127.50 , 126.77, 122.47, 114.53, 114.20, 55.72, 47.42.

N-(1-benzylpiperidin-4-yl)-4-((3-(4-methoxyphenyl) thioureido) methyl) benzamide **(MA3)** Pale yellow powder in a yield (67%), M.P. (188−191), FT-IR: 3441, 3259, 3105, 2920, 2850, 1620, 1539, 1477, 1269, 1180 cm^{-1}, ^1H NMR (400 MHz, DMSO-d6) δ 12.13 (s, 1H, NH), 8.26 (s, 1H, NH), 8.13 (s, 1H, NH), 7.74–7.49 (m, 11H, CH), 6.84 (s, 2H, CH), 5.17 (s, 1H, CH), 4.79 (s, 2H, CH_2), 4.14 (d, 2H, CH_2), 3.73 (s, 3H, CH_3), 1.29 (s, 4H, CH_2), 0.86 (s, 4H, CH_2).

N-((1H-indol-3-yl) methyl)-4-((3-(4-methoxyphenyl) thioureido) methyl) benzamide **(MA4)**

Red powder in a yield (61%), M.P. (127−129), FT-IR: 3259, 3248, 3047, 2924, 2832, 1689, 1612, 1543, 1508, 1284,

1246, 1168 cm-1, ^{1}H NMR (500 MHz, DMSO-*d6*) δ 10.89 (s, 1H, NH), 9.47 (s, 1H, NH), 8.72 (s, 1H, NH), 8.00 (s, 1H, NH), 7.82 (d, 2H, CH), 7.63 (d, 1H, CH), 7.35 (d, 3H, CH), 7.27 (s, 1H, CH), 7.23 (d, 2H), 7.06 (m, 1H, CH), 6.96 (m, 1H, CH), 6.90 (d, 2H, CH), 4.75 (d, 2H, CH_2), 4.62 (d, 2H, CH_2), 3.72 (s, 3H, CH_3).

N-(5-chloropyridin-2-yl)-4-((3-(4-methoxyphenyl) thioureido) methyl) benzamide **(MA5)**

White powder in a yield (43%), M.P. (181–184), FT-IR: 3286, 3251, 3043, 2924, 2854, 1651, 1608, 1597, 1527, 1508, 1469, 1296, 1242, 1168 cm^{-1}, ^{1}H NMR (500 MHz, DMSO-*d6*) δ 10.07 (s, 1H, NH), 9.48 (s, 1H, NH), 8.01 (t, 1H, NH), 7.89 (d, 2H, CH), 7.65 (d, 2H, CH), 7.42 (d, 2H, CH), 7.24 (d, 2H, CH), 6.91 (d, 3H, CH), 4.79 (s, 2H, CH_2), 3.73 (s, 3H, CH_3). ^{13}C NMR (126 MHz, DMSO-*d6*) δ 181.76, 165.45, 157.26, 156.00, 143.50, 138.32, 133.87, 132.64, 127.96, 127.49, 126.78, 122.48, 114.53, 114.20, 55.71, 47.41.

N-(benzo[d]thiazol-2-yl)-4-((3-(4-methoxyphenyl) thioureido) methyl) benzamide **(MA6)**

White powder in a yield (59%), M.P. (159–162), FT-IR: 3398, 3344, 3051, 2931, 2839, 1639, 1612, 1597, 1535, 1504, 1446, 1280, 1238, 1184 cm^{-1}, ^{1}H NMR (400 MHz, DMSO-*d6*) δ 12.87 (s, 1H, NH), 9.58 (s, 1H, NH), 8.13 (d, 1H, NH), 8.03 (d, 1H, CH), 7.79 (d, 2H, CH), 7.65 (d, 1H, CH), 7.49 (d, 2H, CH), 7.34 (t, 2H, CH), 7.28 (d, 2H, CH), 6.94 (d, 2H, CH), 4.84 (d, 2H, CH_2), 4.03 (s, 3H, CH_3).

Electronic supplementary information regarding IR and NMR spectra available

Cancer Cell Line Study

Several studies showed that SIRT2 has an inhibitory role in the growth of multiple cancers such as colorectal cancer.[30] The colon cancer (SW480) cell line was used in the *in vitro* MTT assay for the synthesized molecules. The preliminary MTT assay indicated a promising cytotoxic activity for final compounds (**MA1—MA6)** with a low micromolecular half maximal inhibitory concentration (IC_{50}) activity compared with the cytotoxic activity of the well-known sirtuin enzyme inhibitors selisistat and AGK2 that have IC_{50} of (2.5 μM) and (2.0 μM), respectively (Table 3).

Table 3. **The IC_{50} values for final compounds and controls against colon cancer cells (SW480)**

Code	IC_{50} (μM)
Selisistat	2.5 ± 0.015
AGK2	2.0 ± 0.015
MA1	1.3 ± 0.010
MA2	1.0 ± 0.016
MA3	1.5 ± 0.057
MA4	1.2 ± 0.016
MA5	3.5 ± 0.010
MA6	1.2 ± 0.057

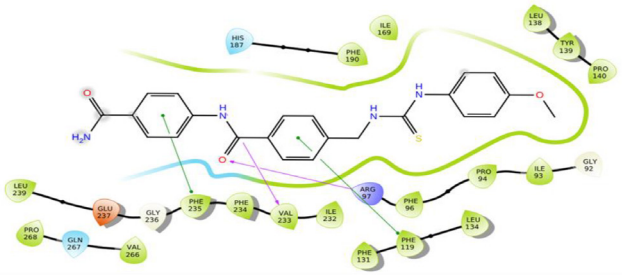

Fig. 2 **The 2D interaction of compound MA2 and SIRT2.**

Discussion

Molecular Docking Study

The virtual interaction of the most active compound **MA2** with SIRT2 indicated that the two-benzene moieties were forming a π-π interaction with PHE119 and PHE235 (Figure 2). The amide carbonyl group that links the two benzene rings forms a hydrogen bond with ARG97. Most interestingly, there is a hydrogen bond formed between VAL233 and the middle amide nitrogen moiety. These interactions are identical to the interaction of reference compound which indicates that compound **MA2** exhibit elegant fitting into the active site of the SIRT2 protein. These superior virtual interaction between **MA2** with SIRT2 might explains its promising antiproliferative activity.

ADMET Study

According to Table 2, none of the final compounds described have a rotating functional group that might be converted into a harmful or undesirable metabolite, following the rule of five (no more than 5 H-bond donors, no more than 10 H-bond acceptors, M. Wt. less than 500, and log *P* less than 5), also the rule of three (Jorgensen's criteria) for oral absorption. The rotating functional groups (rtvFG) of AGK2 can cause toxicity or break down into different compounds. Compound **MA2**, does not show any violation regarding the rule of five indicating the exhibition of an acceptable physicochemical properties profile. Also **MA2** has no rotating functional group and an showed an acceptable percentage of oral absorption.

Cancer Cell Growth Inhibitiion Study

As predicted by the virtual docking studies, cell line anticancer activity of the final compounds revealed that **MA1, MA2, MA3, MA4** and **MA6** have the lowest IC_{50} when compared to selisistat and AGK2 (Table 3). Compound **MA2** shows a lower IC_{50} (1.0 ***μM***), which is slightly lower than reference compounds.

Conclusions

Novel derivatives of thiourea-containing moiety were developed using structure-based and ligand-based drug design strategies for targeting Sirtuin enzymes. The docking study assumed that the designed molecules interact with Sirtuin enzymes through diversified interactions with reasonable docking scores. The final products were synthesized and characterized by FT-IR, ^{1}H-NMR, and ^{13}C-NMR spectroscopy. The antiproliferative activity against colon cancer cells (SW480) denoted that final compounds **MA1—MA6** have a promising antiproliferative activity which is comparable to the activity of well-known SIRT inhibitors of selisistat and AGK2. The promising molecules' preliminary cytotoxicity results might open the avenue for the discovery of new antiproliferative agents.

Electronic Supplementary Information

The following supporting information can be downloaded at:

2D interation for final compound with SIRT2 protein (Figures S1-S6), IR spectra spectra for synthesized compounds (Figures S7-S13), ^{1}H-NMR spectra for synthesized compounds (Figures S14-S20), ^{13}C-NMR spectra for synthesized compounds (Figures S21-S23), IC_{50} plot for reference and final compounds (Figures S24-S31).

Acknowledgments

This work is partially supported by the College of Pharmacy, University of Baghdad

Conflict of Interest

The authors declare that they have no conflict of interest.

References

1. Debela, D.T.; Muzazu, S.G.Y.; Heraro, K.D.; Ndalama, M.T.; Mesele, B.W.; Haile, D.C.; et al. New approaches and procedures for cancer treatment: Current perspectives; SAGE Publications Ltd: 2021.
2. Al-Hamashi, A.A.; Koranne, R.; Dlamini, S.; Alqahtani, A.; Karaj, E.; Rashid, M.S.; et al. A new class of cytotoxic agents targets tubulin and disrupts microtubule dynamics. Bioorganic Chemistry Academic Press Inc.: 2021, 116.
3. Saeed, A.M.; Al-Hamashi, A.A.A. Molecular Docking, ADMET Study, Synthesis, Characterization, and Preliminary Antiproliferative Activity of Potential Histone Deacetylase Inhibitors with Isoxazole as New Zinc Binding Group. Iraqi Journal of Pharmaceutical Sciences University of Baghdad-College of Pharmacy: 2023, 32, 188–203.
4. Davalos, V.; Esteller, M. Cancer epigenetics in clinical practice. CA: A Cancer Journal for Clinicians Wiley: 2023, 73(4), 376–424.
5. Wu, Y.; Sarkissyan, M.; Vadgama, J. V. Epigenetics in breast and prostate cancer. Methods in Molecular Biology Humana Press Inc.: 2015, 1238, 425–466.
6. Mohammed, N.M.; Mohammed, M.H.; Abdulkhaleq, Z.M. Docking Study, Synthesis, Characterization and Preliminary Cytotoxic Evaluation of New 1,3,4-Thiadiazole Derivatives. J Contemp Med Sci | n.d., 9(4), 271–279.
7. Ramaiah, M.J.; Tangutur, A.D.; Manyam, R.R. Epigenetic modulation and understanding of HDAC inhibitors in cancer therapy; Elsevier Inc.: 2021.
8. Kulthinee, S.; Yano, N.; Zhuang, S.; Wang, L.; Zhao, T.C. Critical Functions of Histone Deacetylases (HDACs) in Modulating Inflammation Associated with Cardiovascular Diseases; MDPI: 2022, 471–485.
9. Mohessen Mosa, H.; Abed, A.; Al-Hamashi, A. Oncology and Radiotherapy© Design, synthesis, and antiproliferative activity evaluation of novel N-hydroxyurea derivatives as possible dual HDAC-BET inhibitors; 2024.
10. Roshdy, E.; Mustafa, M.; Shaltout, A.E.R.; Radwan, M.O.; Ibrahim, M.A.A.; Soliman, M.E.; et al. Selective SIRT2 inhibitors as promising anticancer therapeutics: An update from 2016 to 2020; Elsevier Masson s.r.l.: 2021.
11. Mohammad, Y.; Al-Hamashi, A. Oncology and Radiotherapy© Design, synthesis, and evaluation of activity against breast cancer cells of new naphthalene derivatives as potential sirtuin enzymes inhibitors; 2024.
12. Hasan, Y.; Al-Hamashi, A. Identification of Selisistat Derivatives as SIRT1-3 Inhibitors by in Silico Virtual Screening. Turkish Computational and Theoretical Chemistry Turkish Computational and Theoretical Chemistry: 2023, 8(2), 1–11.
13. Mautone, N.; Zwergel, C.; Mai, A.; Rotili, D. Sirtuin modulators: where are we now? A review of patents from 2015 to 2019; Taylor and Francis Ltd: 2020, 389–407.
14. Ronchetti, R.; Moroni, G.; Carotti, A.; Gioiello, A.; Camaioni, E. Recent advances in urea- And thiourea-containing compounds: focus on innovative approaches in medicinal chemistry and organic synthesis; Royal Society of Chemistry: 2021, 1046–1064.
15. Viswas, R.S.; Pundir, S.; Lee, H. Design and synthesis of 4-piperazinyl quinoline derived urea/thioureas for anti-breast cancer activity by a hybrid pharmacophore approach. Journal of Enzyme Inhibition and Medicinal Chemistry Taylor and Francis Ltd: 2019, 34(1), 620–630.
16. Zhao, X.; Allison, D.; Condon, B.; Zhang, F.; Gheyi, T.; Zhang, A.; et al. The 2.5 Å crystal structure of the SIRT1 catalytic domain bound to nicotinamide adenine dinucleotide (NAD +) and an indole (EX527 analogue) reveals a novel mechanism of histone deacetylase inhibition. Journal of Medicinal Chemistry American Chemical Society: 2013, 56(3), 963–969.
17. Yang, L.L.; Wang, H.L.; Zhong, L.; Yuan, C.; Liu, S.Y.; Yu, Z.J.; et al. X-ray crystal structure guided discovery of new selective, substrate-mimicking sirtuin 2 inhibitors that exhibit activities against non-small cell lung cancer cells. European Journal of Medicinal Chemistry Elsevier Masson s.r.l.: 2018, 155, 806–823.
18. Disch, J.S.; Evindar, G.; Chiu, C.H.; Blum, C.A.; Dai, H.; Jin, L.; et al. Discovery of thieno[3,2-d]pyrimidine-6-carboxamides as potent inhibitors of SIRT1, SIRT2, and SIRT3. Journal of Medicinal Chemistry 2013, 56(9), 3666–3679.
19. Friesner, R.A.; Murphy, R.B.; Repasky, M.P.; Frye, L.L.; Greenwood, J.R.; Halgren, T.A.; et al. Extra precision glide: Docking and scoring incorporating a model of hydrophobic enclosure for protein-ligand complexes. Journal of Medicinal Chemistry 2006, 49(21), 6177–6196.
20. Halgren, T.A.; Murphy, R.B.; Friesner, R.A.; Beard, H.S.; Frye, L.L.; Pollard, W.T.; et al. Glide: A New Approach for Rapid, Accurate Docking and Scoring. 2. Enrichment Factors in Database Screening. Journal of Medicinal Chemistry 2004, 47(7), 1750–1759.
21. Mohammed, Z.M.; Abed, A.; Al-Hamashi, A. Molecular Docking, Admet, and Molecular Dynamics Simulation Studies for Molecules with Expected Hdac Inhibition Activity. Gomal Journal of Medical n.d., 22(2), 164.
22. Friesner, R.A.; Banks, J.L.; Murphy, R.B.; Halgren, T.A.; Klicic, J.J.; Mainz, D.T.; et al. Glide: A New Approach for Rapid, Accurate Docking and Scoring. 1. Method and Assessment of Docking Accuracy. Journal of Medicinal Chemistry 2004, 47(7), 1739–1749.
23. Boss, C.; Hazemann, J.; Kimmerlin, T.; Korff, M. Von; Lüthi, U.; Peter, O.; et al. The screening compound collection: A key asset for drug discovery. Chimia Swiss Chemical Society: 2017, 71(10), 667–677.
24. Rajagopal, K.; Kalusalingam, A.; Bharathidasan, A.R.; Sivaprakash, A.; Shanmugam, K.; Sundaramoorthy, M.; et al. In Silico Drug Design of Anti-Breast Cancer Agents. Molecules MDPI: 2023, 28(10).
25. Hussien, M.S.; Al-Hamashi, A.A. Phytosterol Profile in Iraqi Lactuca serriola after Purification and Isolation by Combiflash and HPLC; In Iraqi Journal of Pharmaceutical Sciences; University of Baghdad - College of Pharmacy: 2022, 54–61.
26. Shakeel, A. Thiourea Derivatives in Drug Design and Medicinal Chemistry: A Short Review. Journal of Drug Design and Medicinal Chemistry Science Publishing Group: 2016, 2(1), 10.
27. Shulgau, Z.; Palamarchuk, I.; Sergazy, S.; Urazbayeva, A.; Gulyayev, A.; Ramankulov, Y.; et al. Synthesis, Computational Study, and In Vitro α-Glucosidase Inhibitory Action of Thiourea Derivatives Based on 3-Aminopyridin-2(1H)-Ones. Molecules 2024, 29(15), 3627.
28. Ghosh, A.K.; Shahabi, D. Synthesis of amide derivatives for electron deficient amines and functionalized carboxylic acids using EDC and DMAP and a catalytic amount of HOBt as the coupling reagents. Tetrahedron Letters Elsevier Ltd: 2021, 63.
29. Ghorab, M.M.; Alsaid, M.S.; El-Gaby, M.S.A.; Elaasser, M.M.; Nissan, Y.M. Antimicrobial and anticancer activity of some novel fluorinated thiourea derivatives carrying sulfonamide moieties: Synthesis, biological evaluation and molecular docking. Chemistry Central Journal BioMed Central Ltd.: 2017, 11(1).
30. Li, C.; Zhou, Y.; Kim, J.T.; Sengoku, T.; Alstott, M.C.; Weiss, H.L.; et al. Regulation of SIRT2 by Wnt/β-catenin signaling pathway in colorectal cancer cells. Biochimica et Biophysica Acta - Molecular Cell Research Elsevier B.V.: 2021, 1868(4).

Supplementary IMAGES

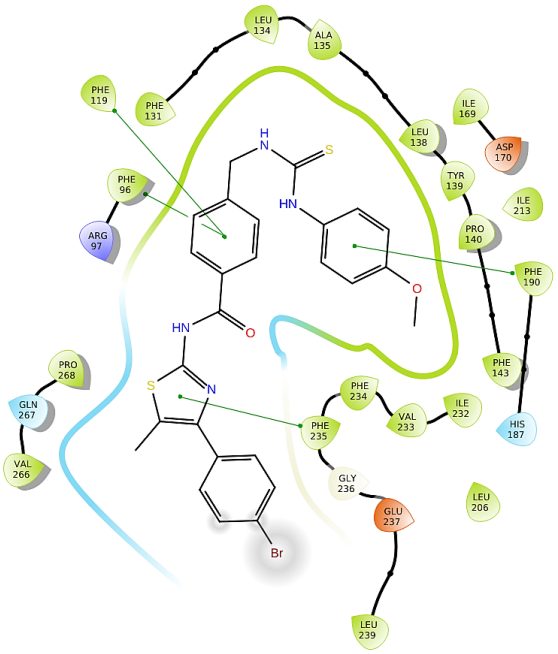

Fig. S1 **The 2D interaction of compound MA1 with SIRT enzyme (PDB: 5YQ0).**

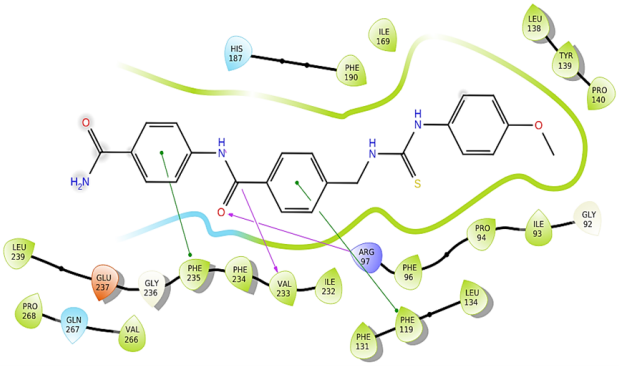

Fig. S2 **The 2D interaction of compound MA2 with SIRT enzyme (PDB: 5YQ0).**

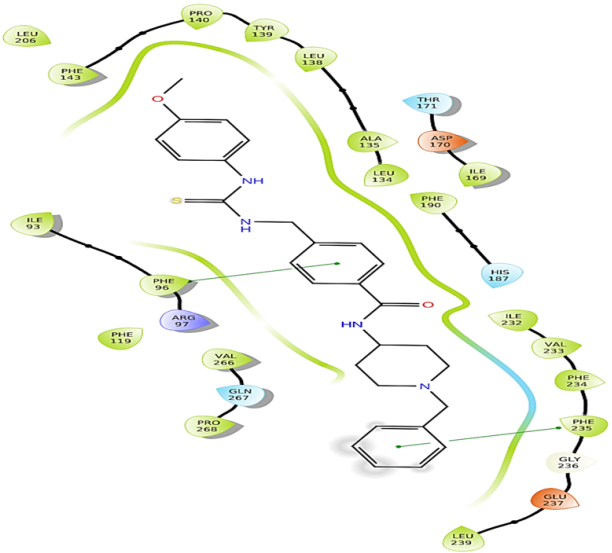

Fig. S3 **The 2D interaction of compound MA3 with SIRT enzyme (PDB: 5YQ0).**

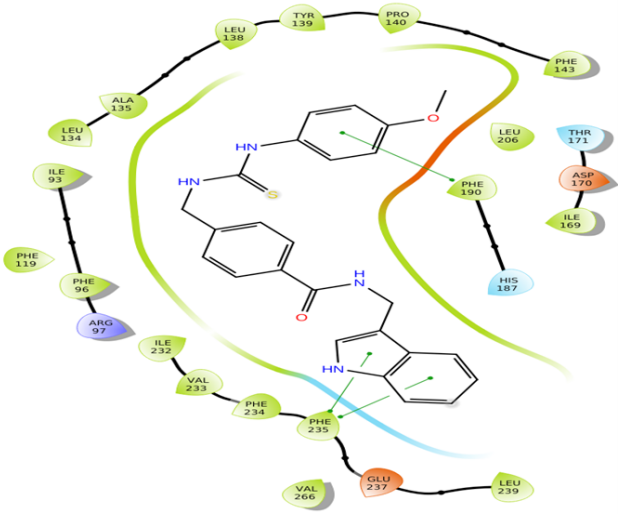

Fig. S4 **The 2D interaction of compound MA4 with SIRT enzyme (PDB: 5YQ0).**

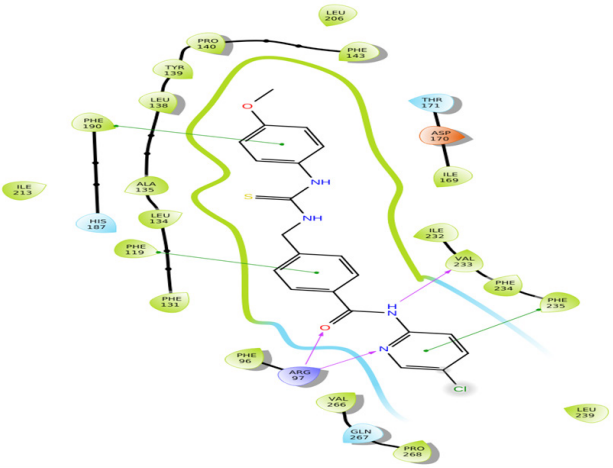

Fig. S5 **The 2D interaction of compound MA5 with SIRT enzyme (PDB: 5YQ0).**

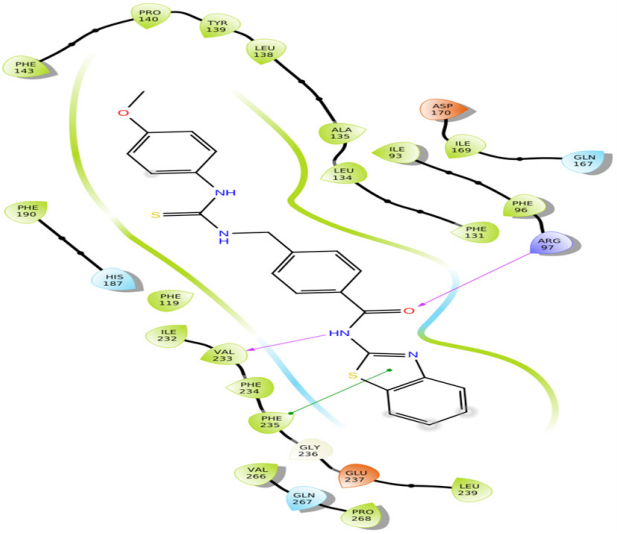

Fig. S6 **The 2D interaction of compound MA6 with SIRT enzyme (PDB: 5YQ0).**

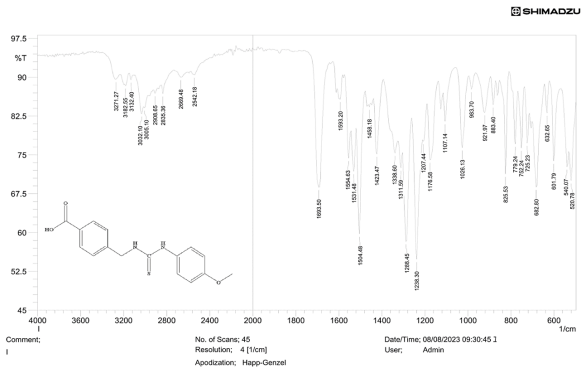

Fig. S7 **IR spectra of intermediate (compound V).**

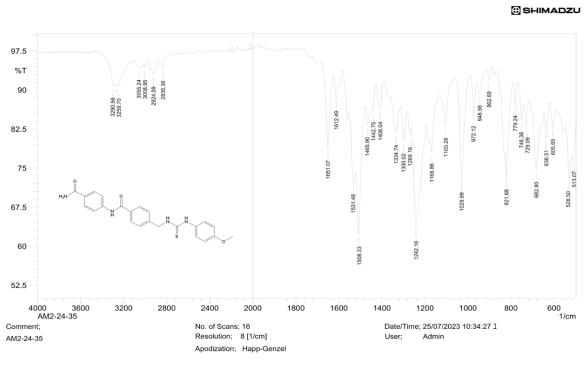

Fig. S8 **IR spectra of compound MA1.**

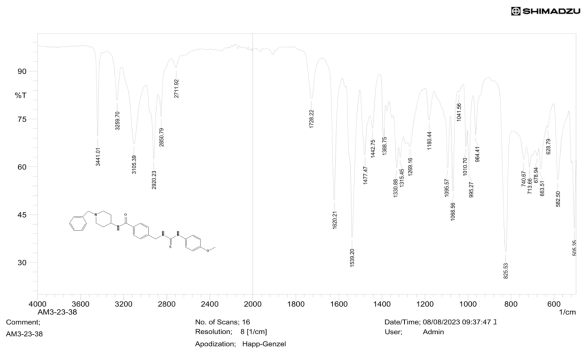

Fig. S9 **IR spectra of compound MA2.**

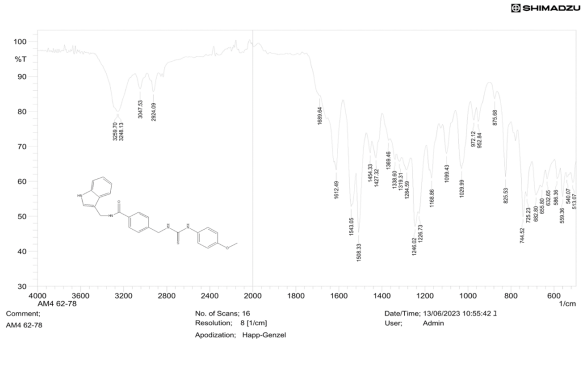

Fig. S10 **IR spectra of compound MA3.**

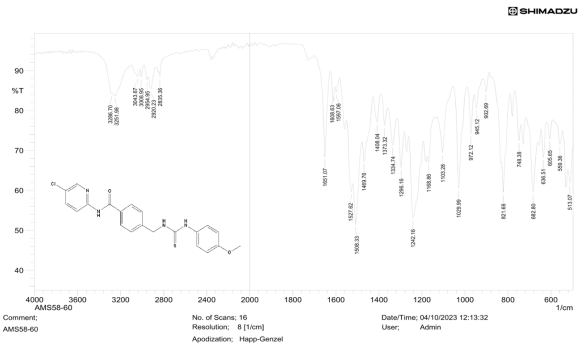

Fig. S11 **IR spectra of compound MA4.**

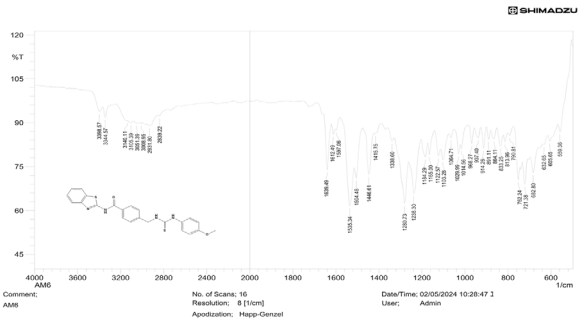

Fig. S12 **IR spectra of compound MA5.**

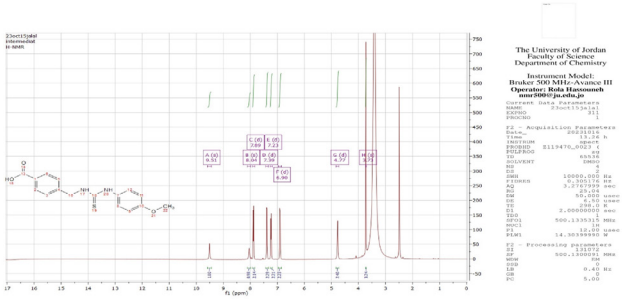

Fig. S13 **IR spectra of compound MA6.**

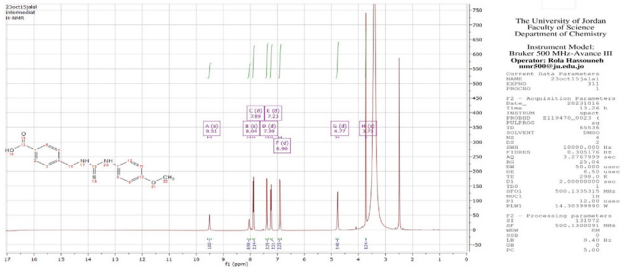

Fig. S14 **^{1}H-NMR spectra of intermediate (compound V).**

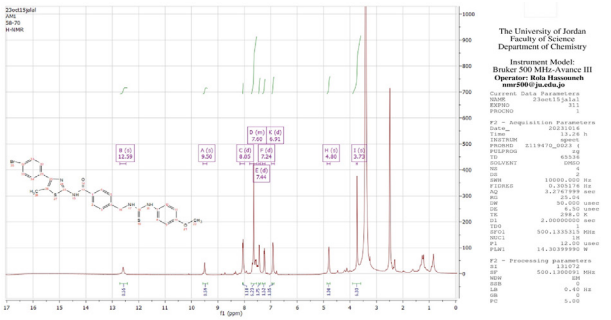

Fig. S15 **^{1}H-NMR spectra of compound MA1.**

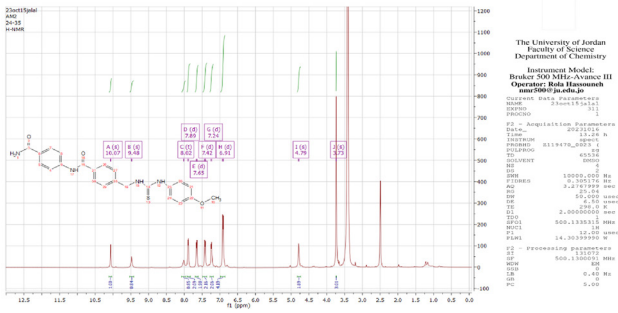

Fig. S16 **^{1}H-NMR spectra of compound MA2.**

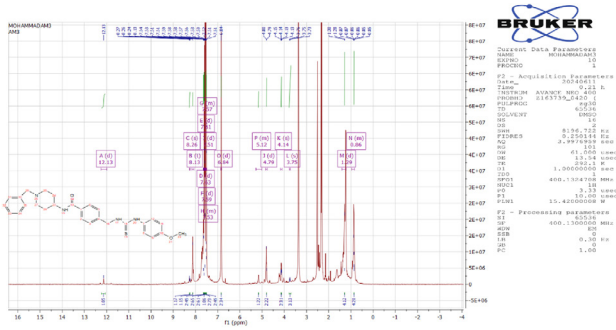

Fig. S17 **^{1}H-NMR spectra of compound MA3.**

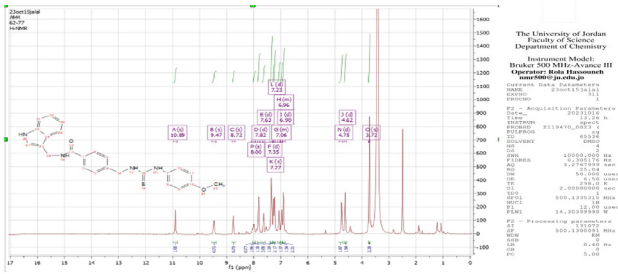

Fig. S18 **^{1}H-NMR spectra of compound MA4.**

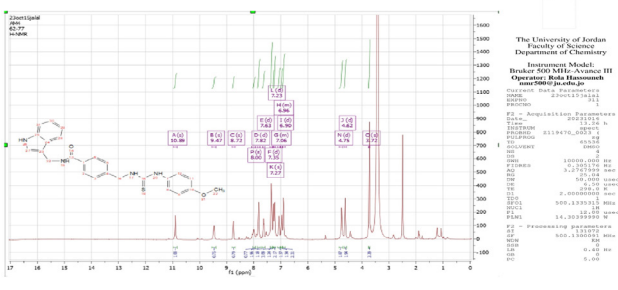

Fig. S19 **^{1}H-NMR spectra of compound MA5.**

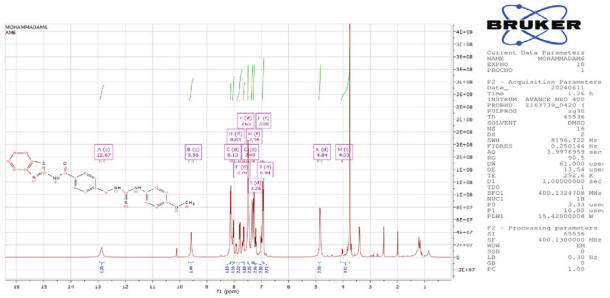

Fig. S20 **^{1}H-NMR spectra of compound MA6.**

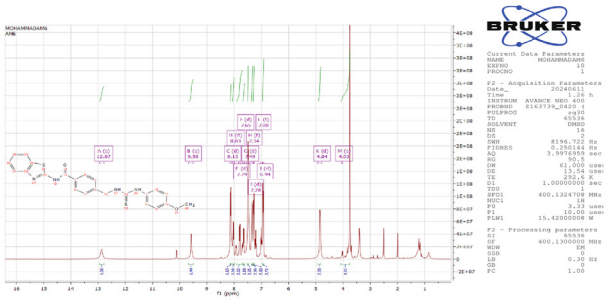

Fig. S20 **^{1}H-NMR spectra of compound MA6.**

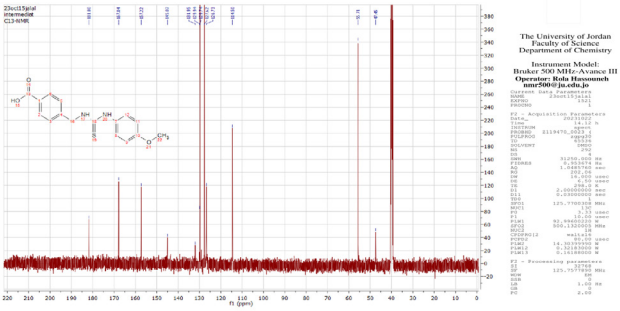

Fig. S21 **^{13}C-NMR spectra of intermediate (compound V).**

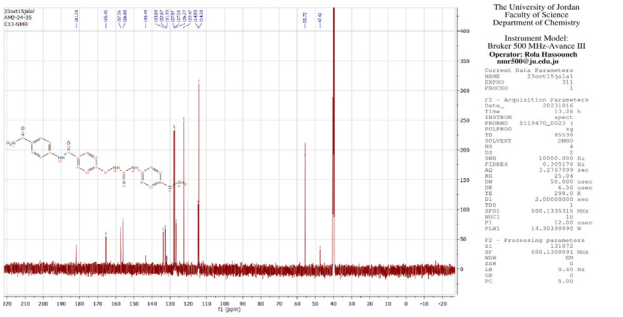

Fig. S22 **^{13}C-NMR spectra of compound MA2.**

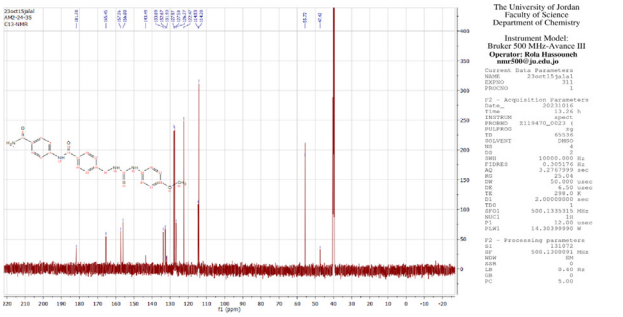

Fig. S23 **^{13}C-NMR spectra of compound MA5.**

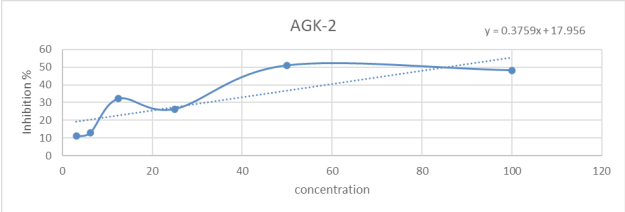

Fig. S24 **IC_{50} plot of AGK2**

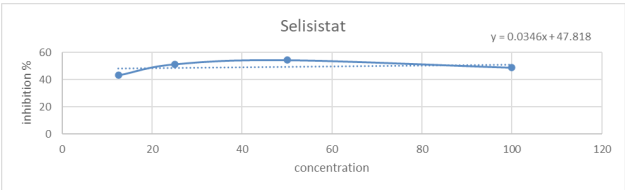

Fig. S25 **IC_{50} plot of Selisistat.**

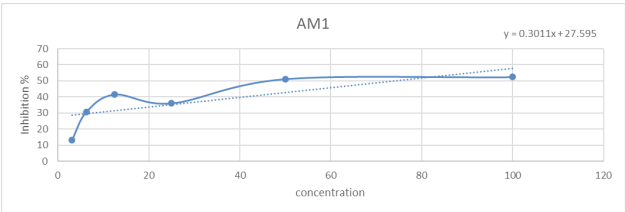

Fig. S26 **IC_{50} plot of compound MA1.**

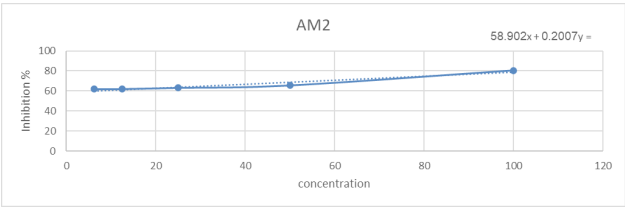

Fig. S27 **IC_{50} plot of compound MA2.**

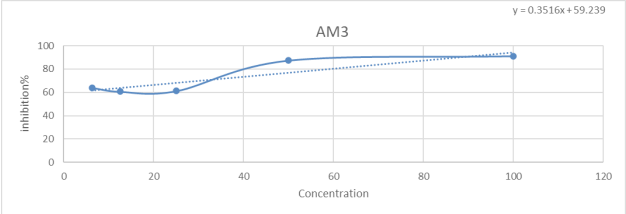

Fig. S28 **IC_{50} plot of compound MA3.**

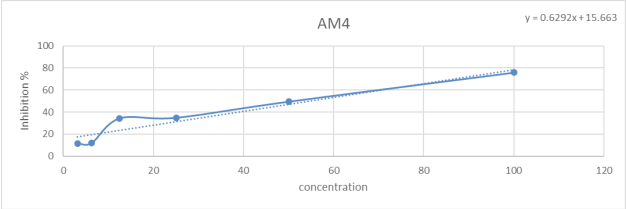

Fig. S29 **IC_{50} plot of compound MA4.**

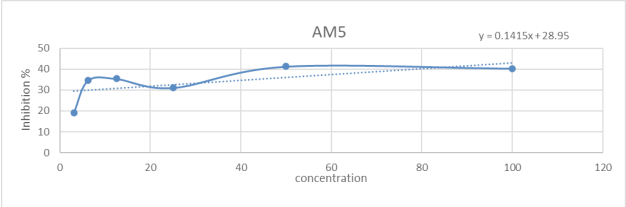

Fig. S30 **IC_{50} plot of compound MA5.**

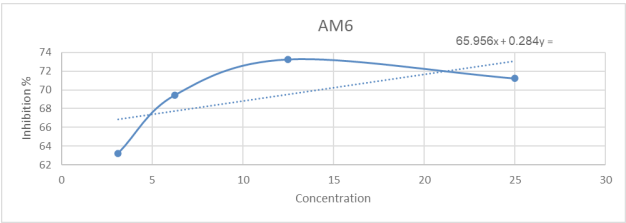

Fig. S31 **IC_{50} plot of compound MA6.**